Geological Magazine

www.cambridge.org/geo

Slowing rates of regional exhumation in the western Himalaya: fission track evidence from the Indus Fan

Peng Zhou[1], Andrew Carter[2], Yuting Li[3] and Peter D. Clift[1,4]

[1]Department of Geology and Geophysics, Louisiana State University, Baton Rouge, LA, 70803, USA; [2]Department of Earth and Planetary Sciences, Birkbeck College, University of London, London WC1E 7HX, UK; [3]Department of Earth, Atmospheric, and Planetary Sciences, Purdue University, West Lafayette, IN, 47907, USA and [4]Research Center for Earth System Science, Yunnan University, Kunming, Yunnan Province, 650091, China

Original Article

Cite this article: Zhou P, Carter A, Li Y, and Clift PD (2020) Slowing rates of regional exhumation in the western Himalaya: fission track evidence from the Indus Fan. *Geological Magazine* **157**: 848–863. https://doi.org/10.1017/S001675681900092X

Received: 26 April 2018
Revised: 12 June 2019
Accepted: 12 July 2019
First published online: 3 October 2019

Keywords:
International Ocean Discovery Program; fission track; erosion; Himalaya; Indus Fan; monsoon

Author for correspondence:
Peter D. Clift, Email: pclift@lsu.edu

Abstract

We use apatite fission track ages from sediments recovered by the International Ocean Discovery Program in the Laxmi Basin, Arabian Sea, to constrain exhumation rates in the western Himalaya and Karakoram since 15.5 Ma. With the exception of a Triassic population in the youngest 0.93 Ma samples supplied from western Peninsular India, apatite fission track ages are overwhelmingly Cenozoic, largely <25 Ma, consistent with both a Himalaya–Karakoram source and rapid erosion. Comparison of the minimum cooling age of each sample with depositional age (lag time) indicates an acceleration in exhumation between 7.8 and 7.0 Ma, with lag times shortening from ~6.0 Myr at 8.5–7.8 Ma to being within error of zero between 7.0 and 5.7 Ma. Sediment supply at 7.0–5.7 Ma was largely from the Karakoram, and to a lesser extent the Himalaya, based on U–Pb zircon ages from the same samples. This time coincides with a period of drying in the Himalayan foreland caused by weaker summer monsoons and Westerly winds. It also correlates with a shift of erosion away from the Karakoram, Kohistan and the Tethyan Himalaya towards more erosion of the Lesser and Greater Himalaya and Nanga Parbat, as shown by zircon U–Pb provenance data, and especially after 5.7 Ma based on Nd isotope data. Samples younger than 5.7 Ma have lag times of ~4.5 Myr, similar to Holocene Indus delta sediments.

1. Introduction

If we are to understand how the evolving climate of Asia has impacted the tectonic development of the Himalaya and Tibetan Plateau, or vice versa, we must use the sedimentary records in basins adjacent to these mountain ranges in order to reconstruct the long-term history of exhumation caused by erosion. Thermochronology measurements on bedrock currently exposed at the surface only provide constraints on the most recent stages of the cooling history of those particular units. By definition, older bedrock has been removed, so the older erosional history can only be reconstructed through study of the sedimentary record. However, interpreting the sedimentary record can be complicated if burial of sediment resets sensitive low-temperature thermochronometers, eliminating the cooling history of the source bedrocks (Carter, 1999). Although higher temperature methods (e.g. muscovite Ar–Ar dating) (White *et al.* 2002; Szulc *et al.* 2006) can be useful in examining past erosion and are resistant to resetting, these have the disadvantage of being less sensitive to changes in the rates of exhumation by erosion, because they require a greater amount of exhumation between isotopic closure and exposure at the surface. Nonetheless, detrital apatite fission track (AFT) thermochronology can also have resolution problems, because single grain ages are often imprecise, especially for young grains with very low track counts.

A number of studies have examined the history of erosion in the Himalaya using the foreland basin sediment record, in particular sedimentary rocks belonging to the Miocene–Pliocene Siwalik Group (Cerveny *et al.* 1989; Ghosh & Kumar, 2000; Bernet *et al.* 2006; Najman, 2006; van der Beek *et al.* 2006; Chirouze *et al.* 2013; Baral *et al.* 2016; Chirouze *et al.* 2015). Although this stratigraphic unit has provided useful information about past patterns and rates of erosion, the quality of information from AFT thermochronology has been limited due to resetting caused by post-deposition burial, especially in the lower parts of the section (van der Beek *et al.* 2006). In addition, the foreland basin sequence at any one particular location will typically reflect the rivers that are flowing from the Himalaya at that point, providing a localized record. Although this may be very useful for examining single rivers, it is often hard to judge how effective each sequence might be in reconstructing erosion at the regional scale. For example, because the trunk Indus River lies on the western edge of the drainage, Siwalik Group rocks in the eastern parts of the catchment provide no information about how its sediment load may have evolved.

CAMBRIDGE UNIVERSITY PRESS

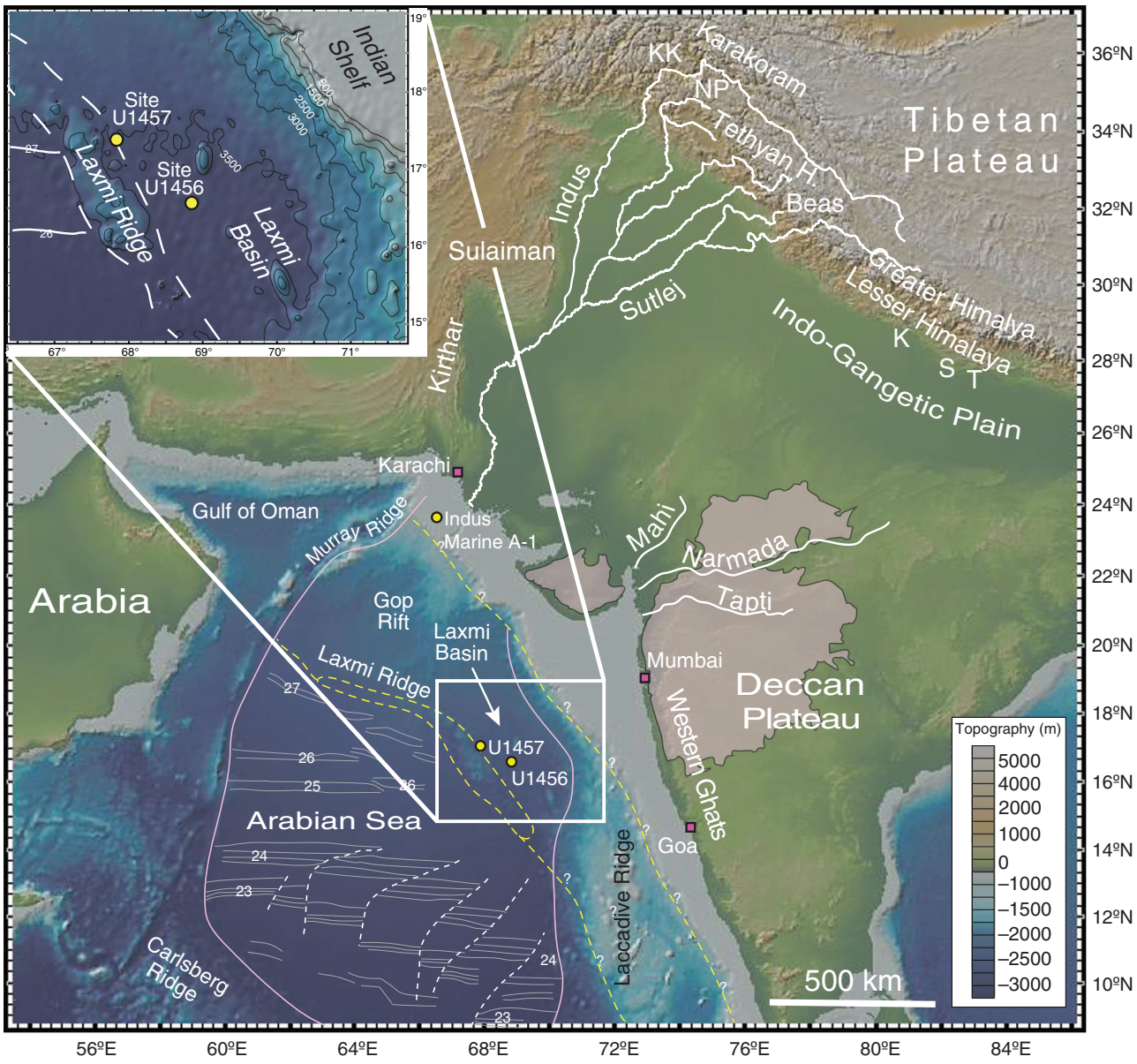

Fig. 1. Shaded bathymetric and topographic map of the Arabian Sea area showing the location of the drilling sites within the Laxmi Basin. Map also shows the primary source ranges and the major tributary systems of the Indus River, as well as smaller peninsular Indian rivers that may have provided material to the drill sites. Magnetic anomalies are from Miles & Roest (1993). KK – Karakoram; NP – Nanga Parbat; K – Karnali; S – Surai Khola; T – Tinau Khola.

In this study, we present AFT data from new scientific boreholes in the western Indian Ocean in order to derive a regional image of changing erosion rates within the western Himalaya since *c.* 15.5 Ma, and in particular after 9 Ma. Use of the International Ocean Discovery Program (IODP) boreholes in the Laxmi Basin (Fig. 1) (Pandey *et al.* 2016*b*) has the advantage that the sediment thickness is low (<1.1 km) and the geothermal gradient is 53 °C km^{-1} and 57 °C km^{-1} at sites U1456 and U1457, respectively (Pandey *et al.* 2016*b*). Although these are high values, the low thickness means that even the base of the section will fall below temperatures required to cause significant annealing or resetting of fission tracks in apatite, i.e. ~60–110 °C (Green, 1989), and therefore the original cooling history of the bedrock sources will be preserved. All but one of the samples were recovered from depths shallower than 722 metres below seafloor (mbsf), implying no more than 38 °C burial temperature at the present maximum burial depth. The deepest sample (U1456E-19R-3, 10–20 cm) was recovered from a depth of 1103 mbsf, but the fission track ages are older than the depositional age, indicating that this too is not reset.

Constraining rates of bedrock source cooling caused by erosion driven by rock uplift can help identify locations of active tectonics and the rates and patterns of mountain growth. However, climate change may also play a role in relation to variations in precipitation rate that are linked to the intensity of the South Asian monsoon. This is known to have varied significantly throughout the Cenozoic (Quade *et al.* 1989; Kroon *et al.* 1991; Prell *et al.* 1992; Gupta *et al.* 2015; Betzler *et al.* 2016). Debate continues concerning the history of strengthening of the South Asian monsoon, but increasingly there is a consensus that the climate began to dry after 8 Ma (Behrensmeyer *et al.* 2007; Singh *et al.* 2011; Clift, 2017),

https://doi.org/10.1017/S001675681900092X Published online by Cambridge University Press

following a period of maximum intensity in Middle Miocene time (Clift *et al.* 2008). It has been suggested that it was the strength of the summer monsoon rains during Middle Miocene time that resulted in rapid exhumation of the Greater Himalaya at that time driven by strong erosion (Clift *et al.* 2008). If that is true, one might predict that the rate of erosion since that time was also coupled with monsoon intensity. However, work within the foreland sedimentary rocks of the Siwalik Group in Nepal shows that the rate of exhumation in the central Nepalese Himalaya remained essentially constant after 8 Ma (van der Beek *et al.* 2006). In contrast, the same study argued that rates of erosion had increased between 8 and 3 Ma in western Nepal, despite the fact that both sections lie within the Ganges drainage system, which is wetter than the Indus Basin considered here (Bookhagen & Burbank, 2006). In contrast, AFT data from Ocean Drilling Program (ODP) sites 717 and 718 on the Bengal Fan showed that rapid rates of exhumation of the bedrock sediment sources to the Ganges–Brahmaputra basin have been ongoing since Middle Miocene time (Corrigan & Crowley, 1990). Reappraisal of this data by van der Beek *et al.* (2006) indicated relatively constant lag times (i.e. the difference between the depositional age and the AFT cooling) since 9 Ma, suggestive of uniform erosion rates.

There are few constraints over how erosion rates might have changed during the Pleistocene Epoch. While some have argued that the onset of northern hemisphere glaciation (NHG) has intensified rates of erosion during the last couple of million years (Métivier *et al.* 1999; Zhang *et al.* 2001; Clift, 2006), other workers, drawing on cosmogenic isotope data (Willenbring & von Blanckenburg, 2010), suggested that continental weathering rates have remained essentially steady-state during the Neogene and especially the Plio-Pleistocene periods. Such an observation does not require faster sediment delivery to the ocean, although this was proposed from a global data compilation implying a steady-state supply of sediment spanning tens of millions of years (Sadler & Jerolmack, 2014). Here we provide the first detailed AFT constraints on erosion rates in the western Himalaya, within the Indus Basin, in order to see whether the temporal evolution in that region mirrors that found in Nepal and in the Ganges–Brahmaputra drainage basin.

Over the period since 15.5 Ma considered by this study, the western Himalaya have experienced significant tectonic changes. The Lesser Himalaya were brought to the surface because of duplexing above the Main Boundary Thrust (MBT) (Mugnier *et al.* 1994; Huyghe *et al.* 2001), coupled with focused erosion since Late Miocene time. There is continued debate about when unroofing of the Lesser Himalaya might have occurred. Early studies suggested that the MBT initiated *c.* 10–11 Ma (Meigs *et al.* 1995) allowing the Lesser Himalayan Duplex to form and be uplifted and then eroded. Work from the Siwalik Group in NW India points to an initial exposure of the Lesser Himalaya at *c.* 9 Ma followed by more widespread exposure after 6 Ma (Najman *et al.* 2009), although this may be only applicable to the Beas River area (Fig. 1). Nd and zircon U–Pb data from IODP sites U1456 and U1457 now suggest initial exposure after 8.3 Ma and widespread unroofing after 1.9 Ma (Clift *et al.* 2019*b*). Other potentially important sources of sediment to the submarine fan include the Nanga Parbat Massif that is located next to the Indus River in the western syntaxis (Fig. 1). Provenance studies from the Indus River downstream of Nanga Parbat indicate that this massif has only limited sediment-generating potential at the present time (Clift *et al.* 2002*b*; Lee *et al.* 2003; Garzanti *et al.* 2005), despite the start of uplift *c.* 6 Ma (Chirouze *et al.* 2015). In contrast, its eastern equivalent (Namche Barwe) is believed to be a major source of sediment to the Brahmaputra (Garzanti *et al.* 2004; Stewart *et al.* 2008). Bedrock thermochronology measurements testify to Nanga Parbat being very rapidly exhumed in the recent geologic past (Zeitler *et al.* 1993), but this does not seem to generate much of the sediment in the river downstream of that point (Alizai *et al.* 2011). Zircon fission track (ZFT) and Nd isotope data in the western part of the Siwalik ranges in Pakistan indicate that this massif and other Himalayan units in the western syntaxis may have become more important as a sediment source after *c.* 6 Ma (Chirouze *et al.* 2015). The sedimentary record in the Indus Fan may have also been affected by large-scale drainage capture. Nd isotope measurements on samples from an industrial drill site on the Indus shelf, as well as limited ODP samples from the upper fan, were used to argue that the eastern tributaries of the Indus River were only captured into the modern system after 5 Ma (Clift & Blusztajn, 2005). However, this is contradicted by combined ZFT and Nd isotope data that support relative stability in drainage patterns but changing rates of erosion in the Himalaya and Karakoram since Miocene time (Chirouze *et al.* 2015).

2. Regional setting

IODP Expedition 355 sampled sediments from the Indus Fan deposited within the Laxmi Basin offshore western India (Fig. 1). Although the Laxmi Basin is separated from the main Arabian Basin by the Laxmi Ridge, the bathymetry of the basin and the orientation of active channels (Mishra *et al.* 2016) indicate that the primary source of sediment to the coring locations would be the Indus River, with lesser input from peninsular rivers such as the Tapti and Narmada. Initial petrographic-based interpretations of the sediments made shipboard during the expedition suggested that there were limited amounts of sediment delivery from western India, and it tended to be found only in the youngest parts of the section (Pandey *et al.* 2016*a*).

The Laxmi Basin itself dates from the latest Cretaceous period when India began to separate from the Seychelles (Bhattacharya *et al.* 1994; Pandey *et al.* 1995). Following the onset of India–Asia collision, *c.* 50–60 Ma (Najman *et al.* 2010; DeCelles *et al.* 2014), the uplift and erosion of the Himalaya have resulted in a huge flux of sediment into the Arabian Sea. Although the Indus Fan is much smaller than the Bengal Fan, it is nonetheless the second largest sediment body on Earth and is believed to have accumulated sediment eroded from the mountains at least since 45 Ma (Clift *et al.* 2001).

Drilling during Expedition 355 recovered a section that penetrated to basement at Site U1457 (Fig. 2), but because of large-scale mass wasting (Dailey *et al.* 2019), the most complete erosional record only spans the last 10.8 Myr, with much of the older sediment either missing, owing to erosion or non-deposition, or not sampled. Coring was undertaken at two sites, Site U1456 in the central part of the Laxmi Basin, as well as at Site U1457 located on the flanks of the Laxmi Ridge (Fig. 1). In general, the sediment at Site U1456 tended to be coarser grained (Fig. 2). The entire sedimentary cover is also more complete at Site U1456 than at Site U1457. The coarse-grained, sandy sediment that forms the focus of this study was taken from both sites and is the product of turbidity current flows. Nonetheless, significant parts of the section are fine-grained

https://doi.org/10.1017/S001675681900092X Published online by Cambridge University Press

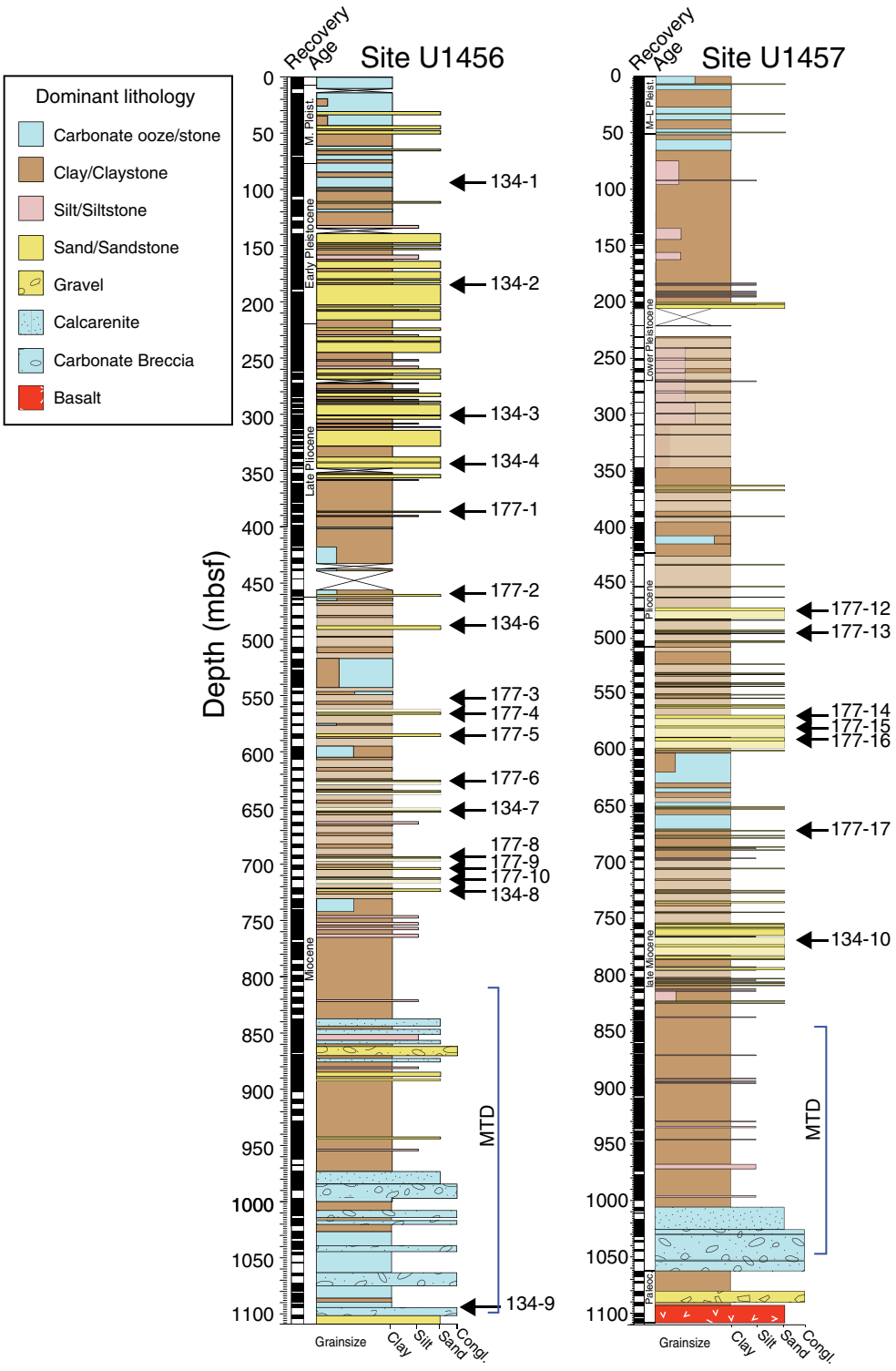

Fig. 2. Simplified lithologic logs of the two drill sites considered in this study. Black arrows show the location of the samples analysed. MTD – Mass Transport Deposit.

muddy facies together with carbonate-rich intervals, and these are interbedded with sandy turbidite material caused by sedimentation on depositional lobes within the middle fan (Fig. 2). There are also interbeds of calcareous-rich pelagic material that reflect times when the main Indus-sourced depocentre was located to the west of the Laxmi Ridge, so that the primary clastic flux from the Indus River was not reaching the drilling area. Because the drilling sites are located above the carbonate compensation depth (CCD), it was possible to date the age of sedimentation using a combination of nannofossil and foraminifera biostratigraphy coupled with magnetostratigraphy that provides a relatively robust age model (Pandey *et al.* 2016*b*). Drilling was able to penetrate a thick mass transport deposit (MTD) deposited just before 10.8 Ma (Calvès *et al.* 2015), but at Site U1456 coring was able to recover a short interval below the MTD, providing a single sample that is substantially older than any of the other sediments recovered and which has been approximately dated at 15.5 Ma (Pandey *et al.* 2016*a*). At Site U1457 all fan sediment

https://doi.org/10.1017/S001675681900092X Published online by Cambridge University Press

Table 1. List of the samples with their depths and calculated depositional ages. Samples also analysed for detrital U–Pb zircon dating by Clift *et al.* (2019*b*) are highlighted

Lab No.	IODP Sample Name	Depositional Age (Ma)	Depth (mbsf)	AFT Minimum Age (Ma)	2σ (Ma)	Number of grains	Zircon U–Pb ages
134-1	U1456A-11H-6 60–69 cm	0.93	97.60	20.70	3.80	24	Yes
134-2	U1456A-26F-3 50–58 cm	1.32	185.91	3.60	0.85	62	
134-3	U1456A-51F-3 100–110 cm	1.56	302.09	3.90	1.40	44	Yes
134-4	U1456A-61F-3 40–50 cm	1.92	345.32	6.50	1.10	45	Yes
177-1	U1456A-70F-2 10–16 cm	3.02	386.73	5.70	1.50	75	Yes
177-12	U1457C-31R-1 94–100 cm	3.17	474.25	5.10	1.80	52	
177-13	U1457C-33R-3 10–17 cm	3.43	499.10	6.40	1.20	49	Yes
177-2	U1456C-45X-3 45–51 cm	3.57	459.09	8.48	0.75	65	
134-6	U1456D-5R-1 12–20 cm	5.72	487.98	9.30	2.20	50	Yes
177-14	U1457C-41R-2 20–26 cm	5.78	572.16	5.91	0.83	46	
177-15	U1457C-42R-1 80–88 cm	5.82	580.40	6.40	1.10	55	
177-16	U1457C-43R-1 55–63 cm	5.87	590.53	9.00	1.20	57	Yes
177-3	U1456D-12R-1 30–36 cm	7.00	556.45	6.60	1.50	52	
177-4	U1456D-13R-1 30–38 cm	7.07	566.35	13.20	7.30	30	Yes
177-5	U1456D-15R-1 55–61 cm	7.28	586.00	15.80	1.90	50	
177-6	U1456D-19R-2 20–26 cm	7.66	625.73	11.90	1.80	40	
177-17	U1457C-51R-4 80–88 cm	7.78	675.16	12.00	3.20	51	
134-7	U1456D-22R-1 73–83 cm	7.84	653.50	15.48	0.97	69	Yes
134-10	U1457C-61R-1 8–18 cm	7.99	769.36	14.00	3.10	42	
177-8	U1456D-26R-2 37–43 cm	8.09	693.78	14.90	1.60	55	
177-9	U1456D-27R-2 100–106 cm	8.15	704.43	16.97	0.98	69	
177-10	U1456D-28R-1 40–46 cm	8.20	711.98	14.20	1.80	72	
134-8	U1456D-29R-2 24–34 cm	8.27	722.60	11.80	5.30	64	Yes
134-9	U1456E-19R-3 10–20 cm	15.58	1102.95	20.20	1.40	75	Yes

pre-dating the mass wasting event had been removed, so our studies are restricted to the section younger than 10.8 Ma at that location.

We apply the AFT thermochronology dating method to this sediment in order to understand how the source rocks that provided material to the Arabian Sea evolved in their cooling and exhumation history since Middle Miocene time. Fission track studies are a well-established method for looking at bedrock unroofing and potentially also sediment provenance if the source regions themselves are sufficiently well defined and if cooling ages are relatively constant in a source area (Laslett *et al.* 1987; Green *et al.* 1989; Carter, 1999). In a complex area like the western Himalaya, cooling ages vary across tectonic blocks and through time, so the interpretation of the AFT ages is contingent on supporting provenance data and cannot be used to constrain provenance by themselves. In this study we draw on zircon U–Pb age data from these same boreholes (Clift *et al.* 2019*b*). Simple comparison of modern bedrock AFT ages and detrital AFT ages in sediments more than around a million years old is not justifiable, because the cooling rates of the bedrock will change on such timescales.

3. Methodology

Low-temperature AFT central ages reflect cooling through 60–110 °C over time scales of 1–10 Myr (Green *et al.* 1989). Fission tracks form continuously through time at an abundance determined by the concentration of ^{238}U in the host apatite grain (Haack, 1977). The method has been widely used and is effective for studying the exhumation history and provenance of shallow-buried sediment (Gallagher *et al.* 1995; Carter, 2007). Samples were taken where suitable sandy material was available at both IODP sites, as shown in Figure 2 and Table 1. Some of the apatites were extracted from the same samples analysed for detrital zircon U–Pb dating by Clift *et al.* (2019*b*).

Following mineral separation, AFT analysis was performed at the London Geochronology Centre based at University College London, UK. Polished grain mounts of apatite were etched with 5N HNO_3 at 20 °C for 20 seconds to reveal the spontaneous fission tracks. Subsequently, the uranium content of each crystal was determined by irradiation, which induced fission in a proportion of the ^{235}U. The induced tracks were registered in mica external detectors. The samples for this study were irradiated in the

https://doi.org/10.1017/S001675681900092X Published online by Cambridge University Press

FRM 11 thermal neutron facility at the University of Munich, Germany. The neutron flux was monitored by including Corning glass dosimeter CN-5, with a known uranium content of 11 ppm, at either end of the sample stack. After irradiation, sample and dosimeter mica detectors were etched in 40 % HF at 20 °C for 25 minutes. Only crystals with sections parallel to the c-crystallographic axis were counted, as these crystals have the lowest bulk etch rate. To avoid biased results through preferred selection of apatite crystals, the samples were systematically scanned and each crystal encountered with the correct orientation was analysed, irrespective of track density. The results of the fission track analysis are presented in Table 2 and online Supplementary Material Table S1. The chi test, used to detect extra Poisson variation, does not show how much over-dispersion is present in the dataset. Therefore, we include the central age and its percentage relative error, because this provides a measure of the extent of age dispersion. It is also useful when there are low track counts (young ages), as the chi test is unreliable under these conditions.

4. Results

Because all samples showed evidence of over-dispersion, we examined the range of single grain AFT ages in each sample using a combination of kernel density estimate (KDE) plots following the method of Vermeesch (2012) and the radial diagrams of Galbraith (1990) (Fig. 3). Plots that combine both types of data presentation are known as abanico plots (Dietze *et al.* 2016). In the radial plots, the single grain ages are plotted away from a central point on the left side of each diagram, with higher accuracy measurements plotted closer to the right-hand curved *y*-axis against which the ages are measured. This approach allows populations of grains with similar ages but varying degrees of uncertainty to be identified as arrays. In this particular study, we focus on the identification of a minimum age population extracted using the algorithm of Galbraith (2005) that clusters in an array and trends towards the *y*-axis on the right-hand side of each diagram. This avoids problems associated with a general purpose, multi-component mixture model that can give a biased estimate of the minimum age towards younger values with increasing sample size. The radial plots show if there is a single source (single array) or multiple sources, if there is more than one array. Figure 3 and Table 2 show samples that have a second age component (P2) as defined by ten or more grains. In all cases the majority of analysed grains defines the minimum age and represents the time at which the dominant bedrock sources cooled through the AFT partial annealing zone (PAZ).

In each case, we also show the calculated depositional age derived from the shipboard biostratigraphy and magnetic stratigraphy (Fig. 3). The minimum ages are older than or concordant with the depositional age, as might be expected in a relatively shallow borehole in which the temperatures are not elevated above those known to reset fission tracks in apatite crystals. All samples have minimum ages less than 20 Ma, and P2 AFT ages are all less than 40 Ma (apart from the youngest sample), post-dating the initial collision of India and Asia. There are particularly noteworthy concentrations of grain ages between 3 and 20 Ma. Fifty per cent of samples have a minimum age younger than 10 Ma. The minimum age gets younger with decreasing depositional age, but not in a systematic way. The age difference between the minimum age and depositional age is <5 Myr for most samples, i.e. short lag times, but increases for samples deposited between 7.84 and 8.2 Ma, as well as 7.07 and 7.28 Ma. The youngest sample (U1456A-11H-6, 60–69 cm) is unlike many of the others in showing significantly older AFT ages (Fig. 3).

The youngest deposited sample is anomalous in having a minimum age population of 20.7 Ma, despite only having been deposited around 930 ka (Fig. 3a). This may be due to the sample containing fewer apatites, with only 24 grains being countable, which is the smallest number out of all samples analysed. This is in strong contrast with the much younger minimum ages of the directly underlying samples. It is only the very oldest sample (~15 Ma, U1456E-19R-3, 10–20 cm) that also has a minimum age of that value, but that sample has a short lag time (Fig. 3x). We can assess the possible impact of low grain numbers on the critical minimum age result in Figure 4. This plot shows that there is no correlation between the number of grains and the minimum age, only reinforcing the fact that samples with low numbers of grains have larger uncertainty in the result, but not causing short lag times.

The core is not altered or veined, and the modern maximum burial temperature of the samples with lag times close to zero is far too cool to have affected the AFT ages. The ages are within error of the depositional age, not resolvably younger, especially considering uncertainties in the depositional age too, although sample U1456D-12R-1 30–36 cm (Fig. 3m) has a minimum age population slightly younger (6.6 ± 1.5 Ma) than the calculated depositional age (7.0 Ma) but within error of that value and need not be reset. Moreover, the young ages are also accompanied by older age populations that are also consistent with the sediment not being thermally reset, as well as with the modern borehole temperatures being well below the apatite PAZ (556 mbsf (29.4 °C) at Site U1456; 572–590 mbsf (32.6–33.6 °C) at Site U1457).

5. Discussion

The fact that all of our AFT ages are relatively young and mostly postdate the widely accepted times of India–Asia collision is a clear indication that they are derived from Himalayan/Karakoram sources supplied by the Indus River and, with the exception of the youngest sample, not from Peninsular India. Ancient rocks of the Indian peninsula have not been substantially deformed and uplifted during Cenozoic time, and basement AFT ages are mostly Jurassic–Cretaceous. Although they range as young as 54 Ma (Kalaswad *et al.* 1993; Gunnell *et al.* 2003), 95 % of the ages measured are older than 100 Ma, averaging 228 Ma (Fig. 5h). This is somewhat older than most of the grain ages in Sample U1456A-11H-6, 60–69 cm (Fig. 3a), but does match the P2 older population in that sample (Table 2). Nonetheless, the minimum age population of 20.7 ± 3.8 Ma requires a Himalaya–Karakoram provenance for 14 of the 24 grains measured. U–Pb zircon ages from this same sample (Clift *et al.* 2019*b*) show that 8 % of the grains date to <200 Ma, requiring derivation from the Indus River, because such zircon ages can only be generated by erosion from Kohistan or Karakoram sources. Zircon grains older than 300 Ma could be from the peninsula or the Tethyan/Greater Himalaya. This youngest sample seems likely to be of mixed provenance, with material from both the Indus and the peninsula. For the other samples, the AFT data argue strongly for the sand at these drilling sites being entirely derived from the Indus River, because they are generally much younger than AFT ages from the western margin of Peninsular India and broadly consistent

https://doi.org/10.1017/S001675681900092X Published online by Cambridge University Press

Table 2. Summary of apatite fission track analytical data

	Lab No	Sample	Dep. Age (Ma)	No. of grains	Dosimeter ρd	Nd	ρs	Ns	ρi	Ni	Pχ^2	RE%	Central Age (Ma)	Minimum Age (Ma)	P2 Age (Ma)
A	134-1	U1456A-11H-6 60–69 cm	0.93	24	1.583	4388	0.798	218	3.858	1440	0	111	61.2±14.9	20.7±3.8	223±28
B	134-2	U1456A-26F-3 50–58 cm	1.32	62	1.583	4388	0.108	308	3.555	11836	0	79	7.3±0.9	3.6±0.9	13.4±1.3
C	134-3	U1456A-51F-3 100–110 cm	1.56	44	1.583	4388	0.191	298	6.856	12192	0	70	6.8±0.9	3.9±1.4	7.2±0.9
D	134-4	U1456A-61F-3 40–50 cm	1.92	45	1.583	4388	0.178	349	5.498	11649	0	35.2	8.1±35.2	6.5±1.1	
E	177-1	U1456A-70F-2 10–16 cm	3.02	75	1.215	3367	0.206	446	4.539	11389	0	54.2	8.2±0.7	5.7±1.5	15.5±2.3
F	177-12	U1457C-31R-1 94–100 cm	3.17	75	1.215	3367	0.171	326	4.710	10359	0	51.5	6.8±0.6	5.1±1.8	12.7±2.1
G	177-13	U1457C-33R-3 10–17 cm	3.43	49	1.215	3367	0.211	313	4.528	8601	0	50.8	7.7±0.8	6.4±1.2	
H	177-2	U1456C-45X-3 45–51 cm	3.57	65	1.215	3367	0.349	474	4.737	9089	0	160	12.9±2.7	8.5±0.8	
I	134-6	U1456D-5R-1 12–20 cm	5.72	50	1.583	4388	0.272	314	6.211	7830	0	42.4	11.2±1.0	9.3±2.2	
J	177-14	U1457C-41R-2 20–26 cm	5.78	46	1.215	3367	0.186	236	3.801	6317	0	180	11.4±3.1	5.9±0.8	
K	177-15	U1457C-42R-1 80–88 cm	5.82	55	1.215	3367	0.179	361	4.073	9719	0	160	7.8±0.8	6.4±1.1	15.9±2.6
L	177-16	U1457C-43R-1 55–63 cm	5.87	80	1.215	3367	0.389	528	5.048	8747	0	12.4	13.7±1.6	9.0±1.2	29.4±1.2
M	177-3	U1456D-12R-1 30–36 cm	7.00	52	1.215	3367	0.241	347	4.004	6997	0	53.8	10.7±1.0	6.6±1.7	17.7±1.7
N	177-4	U1456D-13R-1 30–38 cm	7.07	30	1.215	3367	0.297	124	5.000	2061	2.1	44.7	11.4±1.5	11.4±1.5	
O	177-5	U1456D-15R-1 55–61 cm	7.28	50	1.215	3367	0.362	372	3.718	4683	0	39.2	16.5±1.3	15.8±1.9	
P	177-6	U1456D-19R-2 20–26 cm	7.66	40	1.215	3367	0.546	457	4.714	4931	0	73.4	19.9±2.6	11.9±1.8	28.0±4.7
Q	177-17	U1457C-51R-4 80–88 cm	7.78	51	1.215	3367	0.326	430	4.140	5605	0	40	14.7±1.2	12.0±3.2	19.9±1.6
R	134-7	U1456D-22R-1 73–83 cm	7.84	80	1.583	4388	0.424	799	6.226	12387	0	44.6	18.6±1.2	15.5±0.9	
S	134-10	U1457C-61R-1 8–18 cm	7.99	42	1.583	4388	0.353	468	5.490	7570	0	14.3	16.1±1.0	14.0±3.1	
T	177-8	U1456D-26R-2 37–43 cm	8.09	55	1.215	3367	0.337	403	3.651	5056	0	48.9	18.4±1.7	14.9±1.6	
U	177-9	U1456D-27R-2 100–106 cm	8.15	92	1.215	3367	0309	605	3.710	7958	0	41.8	16.0±1.0	16.9±0.9	
V	177-10	U1456D-28R-1 40–46 cm	8.20	72	1.215	3367	0.499	639	5.203	7453	0	73.3	18.4±1.8	14.2±1.8	21.1±1.9
W	134-8	U1456D-29R-2 24–34 cm	8.27	72	1.583	4388	0.424	639	5.508	9347	0	48.6	19.3±1.4	11.8±5.3	38.8±3.8
X	134-9	U1456E-19R-3 10–20 cm	15.58	75	1.583	4388	0.462	873	4.957	9653	0	55.9	25.9±2.0	20.2±1.4	

Track densities are ($\times 10^6$ tr cm^{-2}) numbers of tracks counted (N) shown in brackets. Analyses by external detector method using 0.5 for the $4\pi/2\,\pi$ geometry correction factor. Ages calculated using dosimeter glass CN-5; (apatite) $\zeta_{CN5} = 338 \pm 5$; calibrated by multiple analyses of IUGS apatite and zircon age standards (Hurford, 1990). Pχ^2 is probability for obtaining χ^2 value for v degrees of freedom, where v = no. crystals – 1. Central age is a modal age, weighted for different precisions of individual crystals (see Galbraith, 1990). Minimum age model after Galbraith (2005). P2 used the peak fitting algorithm of Galbraith & Green (1990) where there are >10 grains.

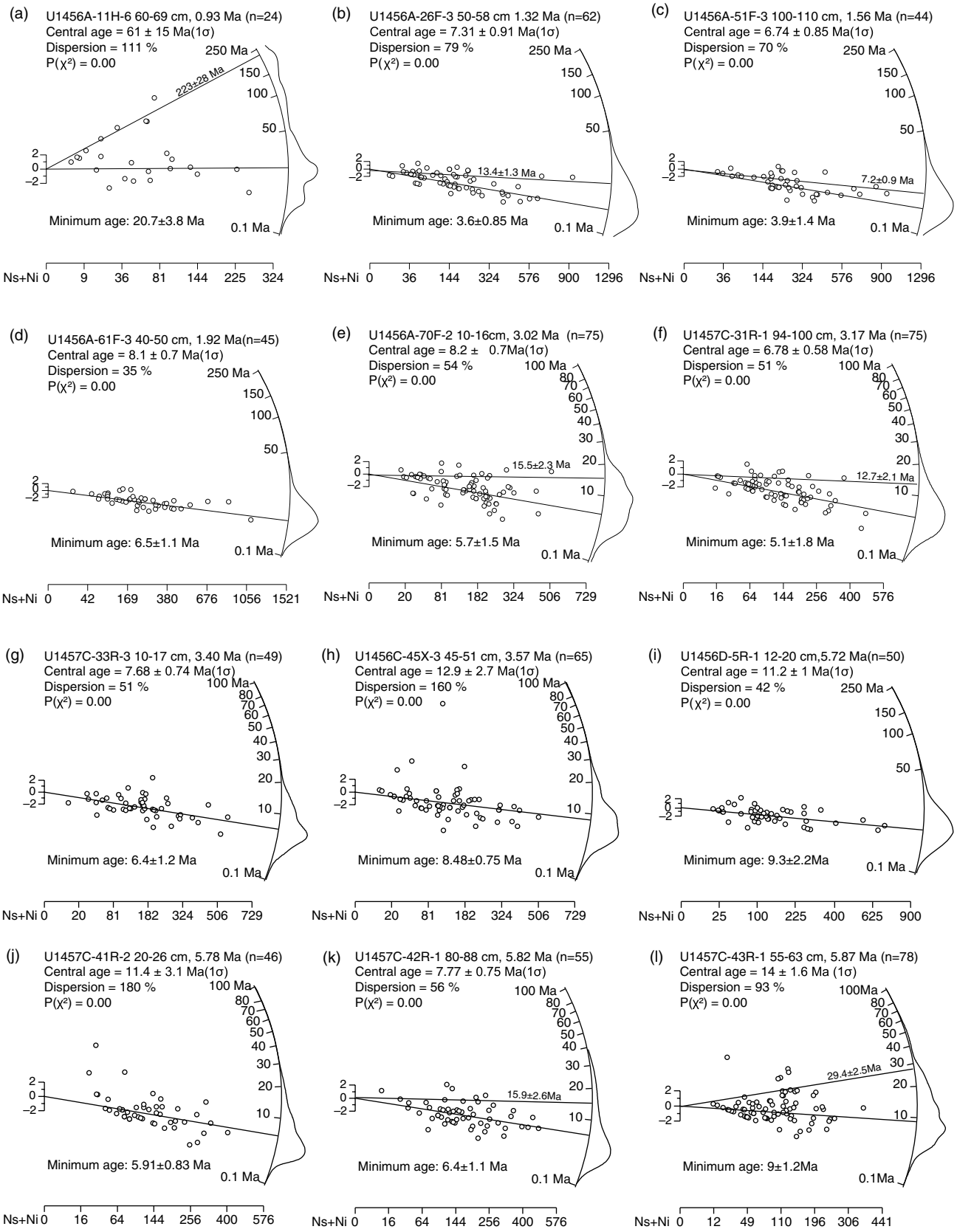

Fig. 3. (a–f) Radial plots and associated KDE spectra (abanico plots) showing the range of apatite fission track ages for each of the samples considered within the study (Galbraith, 1990). Ns – number of spontaneous fission tracks; Ni – number of induced tracks. Single ages are plotted with standard errors according to their precision (1/σ on the *x*-axis). The error attached to each plotted point is standardized on the *y* scale. The value of the age and the 2σ uncertainty can be read off the radial axis by extrapolating lines from point 0,0 through the plotted age. (g–l) Radial plots and associated KDE spectra (abanico plots) showing the range of apatite fission track ages for each of the samples considered within the study (Galbraith, 1990). (m–r) Radial plots and associated KDE spectra (abanico plots) showing the range of apatite fission track ages for each of the samples considered within the study (Galbraith, 1990). (s–x) Radial plots and associated KDE spectra (abanico plots) showing the range of apatite fission track ages for each of the samples considered within the study (Galbraith, 1990).

https://doi.org/10.1017/S001675681900092X Published online by Cambridge University Press

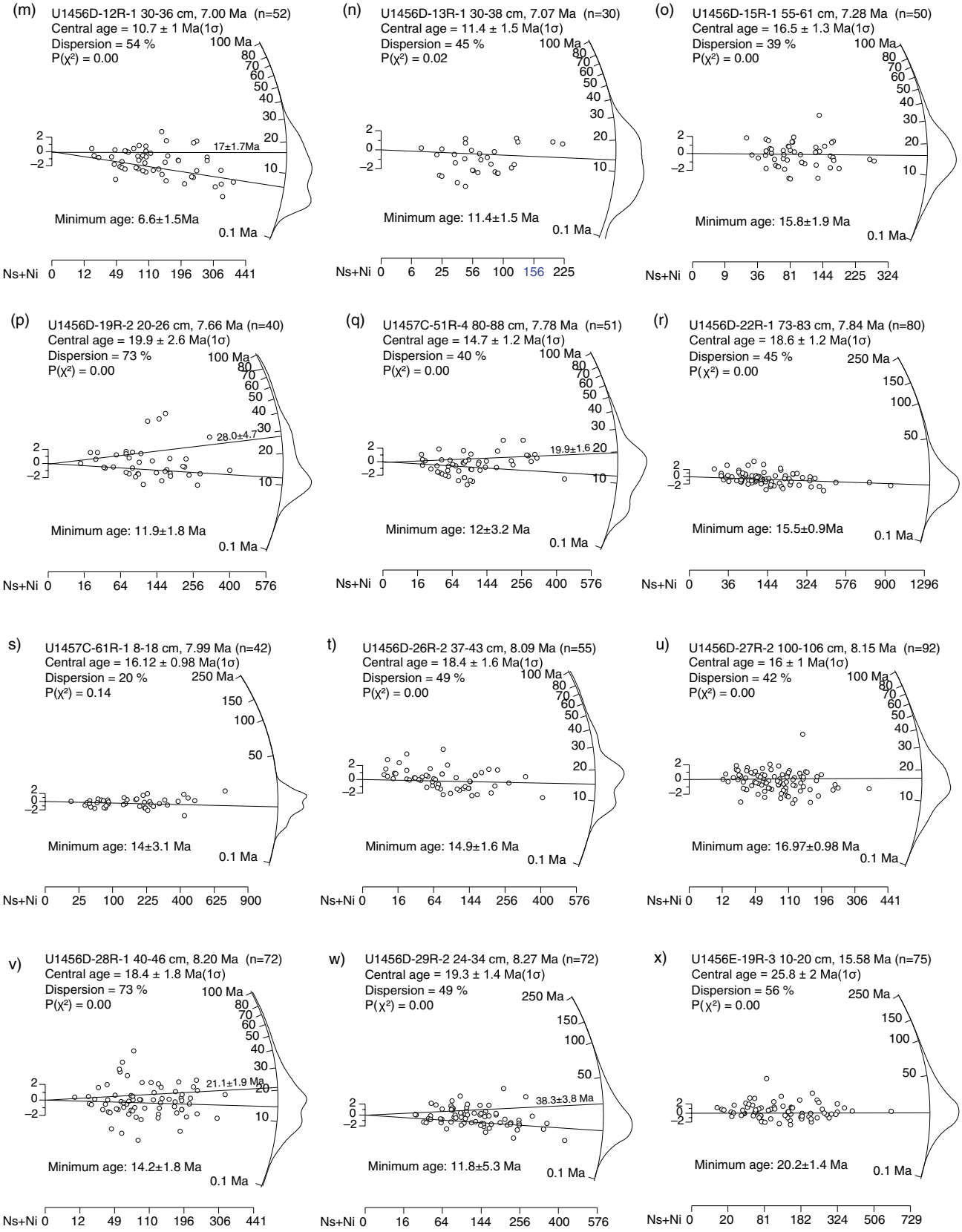

Fig. 3. (*Continued*)

https://doi.org/10.1017/S001675681900092X Published online by Cambridge University Press

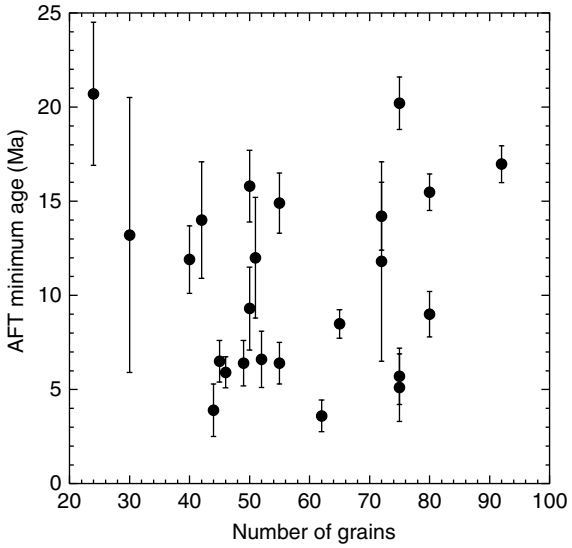

Fig. 4. Cross-plot of numbers of grains compared to minimum ages with 2σ uncertainties displayed. There is no correspondence between the numbers of grains and the minimum age that might bias the result of the lag time analysis.

with the AFT ages derived from sands that are definitely of Indus derivation (Clift *et al.* 2004, 2010).

Some information can also be derived about where the sediments may be coming from within the possible source ranges if we refer to the bedrock data that has been measured onshore, as summarized in Figure 5. Comparison of these sources and detrital data is only valid for the youngest sediments because young bedrock AFT ages do not inform us about the cooling of these sources in the older geologic past, only the cooling of the rocks now exposed. We note that the different ranges within the Indus Basin have a number of distinctive peaks and that some of these are distinct in terms of their AFT age spectra. We note that the Greater and Lesser Himalaya have relatively similar fission track ages, clustering around 3–4 Ma, but with some ranging to *c.* 1 Ma, at least in the Sutlej Valley (Thiede *et al.* 2004), and that these also overlap with ages known from the Karakoram, especially the eastern Karakoram (Wallis *et al.* 2016) and the Yasil Dome lying in the Karakoram immediately north of the Nanga Parbat Massif (Poupeau *et al.* 1991). The Karakoram, however, also has bedrock AFT ages that range to older values, suggestive of earlier exhumation in at least parts of that block, most notably in the west and their continuation into the Hindu Kush (Zhuang *et al.* 2018). The very youngest grains are measured around the Nanga Parbat Massif (Zeitler, 1985), while the oldest are found in the Transhimalayan Ladakh Batholith (Kirstein *et al.* 2009) and Deosai Plateau (van der Beek *et al.* 2009). The Tethyan Himalaya has also yielded older AFT ages in the central Himalaya (Li *et al.* 2015) but has not been dated within the Indus catchment. Uplift and erosion in the mountains around the Indus Suture and to the north of the Greater Himalaya is widely accepted to have initiated earlier and then mostly slowed as the exhumation shifted into the Greater and Lesser Himalayan ranges (Searle, 1996).

Although many of the measured fission tracks at Nanga Parbat have ages of less than 1 Ma (Zeitler *et al.* 1989), clearly this could not have been the case before 1 Ma, when the fastest cooled grains must have had ages within error of or older than 1 Ma. Lag times could, however, have been short prior to 1 Ma. Consequently, direct comparison of the modern bedrock with the detrital ages in old sediments is not appropriate for most of our samples. Because the cooling rates of bedrock sources change on timescale of $>10^6$ yr, source lag times need not have been constant in the geologic past. Different, higher temperature thermochronometers can constrain exhumation rates during those earlier times and provide clues about lag times. We can, however, deduce that because many of the grains' AFT ages are relatively young (<15 Ma) and their lag times are short, they were probably derived from fast-exhuming sources in the Himalaya, Nanga Parbat or Karakoram (Zeitler *et al.* 1993; Zhuang *et al.* 2018), rather than in Kohistan, the Transhimalaya or Tethyan Himalaya where uplift and exhumation were mostly older. The cooling histories of these latter sources imply that their AFT lag times would be mostly long during Late Miocene–Present times (Fig. 5) (Krol *et al.* 1996; Searle, 1996; Kirstein *et al.* 2009). Although some young AFT ages <6.3 Ma have been recorded in the Ladakh Transhimalayan Batholith along the Shyok Suture (Kirstein *et al.* 2009), these represent quite a small part of that tectonic block. Zircon U–Pb ages from the same IODP sites imply that the Transhimalaya has not been a dominant source during the period targeted by this study (maximum of 28 % at 15.5 Ma, and this is likely a large overestimate because the Karakoram and Transhimlaya overlap in zircon U–Pb ages) (Clift *et al.* 2019*b*).

The prevalence of short AFT lag times implies rapid exhumation in the dominant sediment-producing sources close to the time of sedimentation. The AFT data require that little sediment was stored for significant periods of geologic time between erosion in the mountain sources and sedimentation on the Indus submarine fan because the difference/lag between minimum ages and deposition is typically <4 Myr (75 % of samples), representing an upper limit to the storage time. The lag time of a grain largely represents the time between cooling and erosion. While the lag time also includes time spent during sediment transport, study of the Quaternary Indus system indicates transport times of no more than $\sim10^5$ yr for the bulk of the sediment delivered to the deep basin (Clift & Giosan, 2014). Some of the sediment may be recycled from foreland basin sedimentary rocks of the Siwalik Group, and this would introduce an additional lag into the sediment transport history. Secondary AFT age populations between 15 and 38 Ma (Table 2) would fit with this type of recycling. We can discount that these older ages are coming from direct erosion of the slower cooled Ladakh Batholith or Tethyan Himalaya because heavy mineral studies (Garzanti *et al.* 2005), trace-element characteristics of detrital amphiboles (Lee *et al.* 2003) and zircon U–Pb ages (Alizai *et al.* 2011) from the trunk Indus River close to the Himalayan front show dominance by the Karakoram (especially the Southern Karakoram Metamorphic Belt) over other sources in the modern upstream basin. That the AFT ages in Siwalik Group sedimentary rocks themselves have not been entirely reset during burial is known from studies in central Nepal (van der Beek *et al.* 2006), and these ranges could thus be a source of the older AFT ages measured. Quantifying the amount of recycling out of the Siwalik Ranges is impossible for our data, because older grains could come from slow cooling sources or the Siwalik Group. However, the high abundance of short lag time grains suggests that the degree of this recycling cannot be too large. Rates of incision in modern gorges cutting the Siwalik Group in Nepal have been used to estimate that they account for no more than 15 % of the total flux (Laveé & Avouac, 2001), while an isotope-based mass balance

https://doi.org/10.1017/S001675681900092X Published online by Cambridge University Press

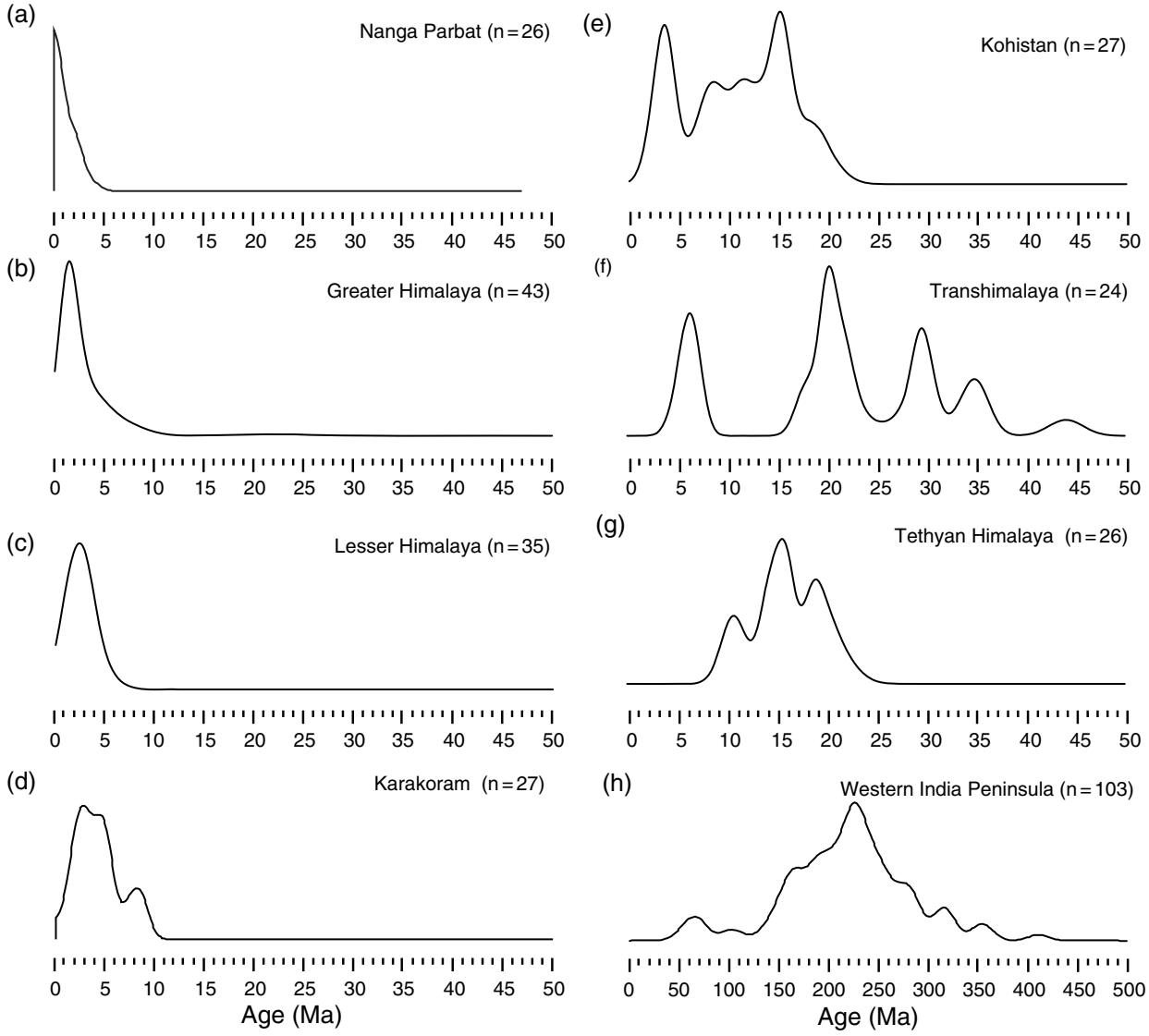

Fig. 5. KDE plots for the apatite fission track central ages of potential bedrock sources within the headwaters of the Indus Basin. Nanga Parbat data are from Warner (1993) and Zeitler (1985). Greater Himalaya data are from Kumar *et al.* (1995), Jain *et al.* (2000) and Thiede *et al.* (2004). Lesser Himalaya data are from Thiede *et al.* (2004) and Vannay *et al.* (2004). Karakoram data are from Foster *et al.* (1994), Zeitler (1985), Wallis *et al.* (2016) and Poupeau *et al.* (1991). Kohistan data are from Zeitler (1985) and Zeilinger *et al.* (2001). Transhimalaya data are from Kirstein *et al.* (2009, 2006) and Clift *et al.* (2002*a*). Tethyan Himalaya data are from Li *et al.* (2015) and A. Carter (unpub. data, UCL, 2017). Indian Peninsula data are from Gunnell *et al.* (2003) and Kalaswad *et al.* (1993).

for the Ganges basin indicates <10 % of the mass flux in that drainage is from the Siwalik Group (Wasson, 2003). A contribution of that order to the Indus Basin would be consistent with the AFT data presented here. The AFT data by themselves cannot resolve erosion from the Siwaliks, as they share older AFT ages with sources in the Tethyan Himalaya, Kohistan and Transhimalaya.

On shorter timescales if sediment was being buffered on the floodplains, in the delta or on the continental shelf, then this is expected to have occurred only for a short amount of time, essentially tens of thousands of years (Li *et al.* 2019). Storage and recycling on million-year timescales would have resulted in longer lag times. When the lag times of our samples are 3–4 Myr some of this time must have been spent during transport. With the exception of the storage and recycling via Siwalik Group foreland sequences discussed above, the assumption is that most of this time would have been spent undergoing rock uplift prior to exposure and erosion, because estimates of transport time in the Quaternary Indus are just 10^5 yr for the bulk of the sediment delivered to the deep basin (Clift & Giosan, 2014). Modern bedrock AFT data from the Greater and Lesser Himalaya and Karakoram indicate this order of lag time at the present day (Fig. 5), without factoring in much additional transport time. Our data are broadly consistent with the idea of rapidly uplifting mountains being strongly eroded and so supplying most of the sediment into the Indus River during the period of study since 15.5 Ma.

Combined Nd isotope and detrital zircon U–Pb age data from bulk sediment samples from sites U1456 and U1457 show that there was a change in provenance starting at *c.* 5.7 Ma (Clift *et al.* 2019*b*). This analysis indicates more material coming from the Greater and Lesser Himalaya and relatively less from the Karakoram after this time. The range of lag times in sediments younger than 7.0 Ma is similar to that found in the Indus delta during the phase of strong summer monsoon in early Holocene

https://doi.org/10.1017/S001675681900092X Published online by Cambridge University Press

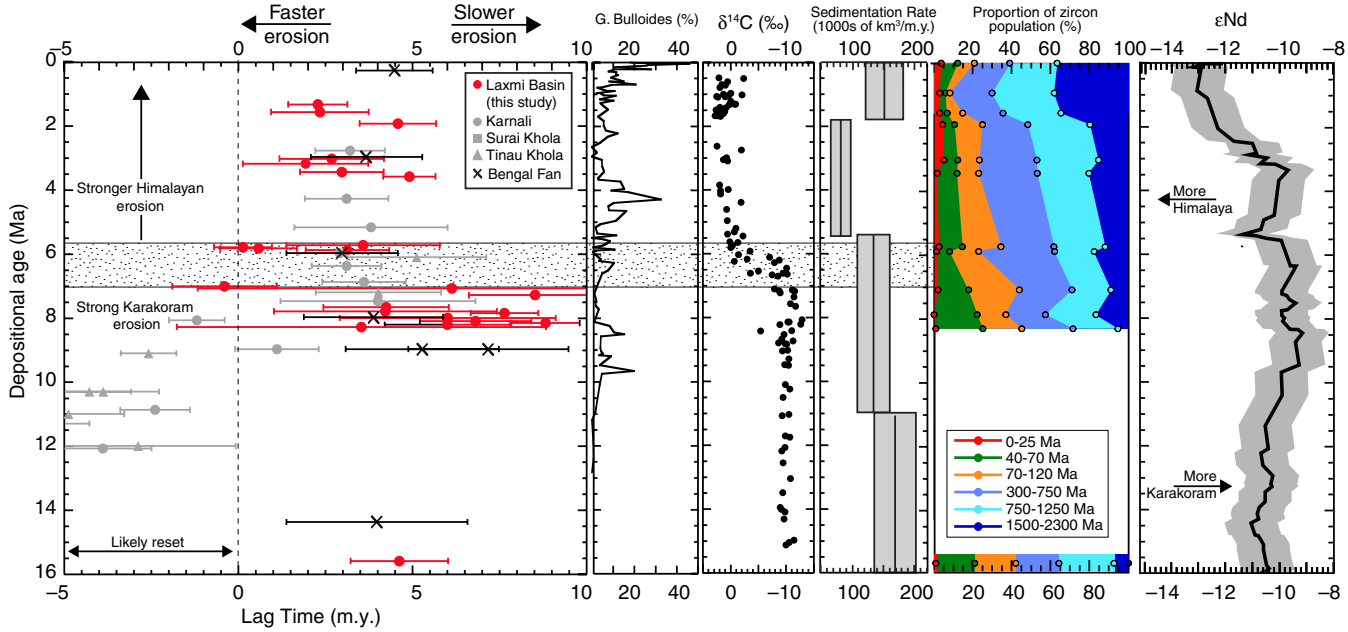

Fig. 6. Lag time plot of detrital apatite fission track minimum ages showing the lag time between the cooling and depositional ages. Note the minimum lag time achieved between 9 and 6 Ma. Siwalik data from Nepal are from van der Beek *et al.* (2006); Bengal Fan data are from Corrigan & Crowley (1990). Monsoon records of *G. bulloides* are from Huang *et al.* (2007); foreland basin $\delta^{14}C$ record is from Quade *et al.* (1989). Sediment budget for the Indus Fan is from Clift (2006). Evolution in the age spectra of zircon U–Pb ages and ϵ_{Nd} values are from Clift *et al.* (2019*b*). Stippled area shows the time of the climatic transition to drier conditions in the foreland basin.

time, i.e. 2–5 Myr (Fig. 6), when the provenance constraints indicate that these sediments were preferentially derived from Greater and Lesser Himalayan sources (Clift *et al.* 2019*b*). In contrast, sediments older than 7.0 Ma have longer lag times (3.5–8.8 Myr, average 6.0 Myr) and are inferred to be more derived from the Karakoram, based on their zircon U–Pb age spectra (Fig. 6) (Clift *et al.* 2019*b*). The fact that lag times of pre-7.0 Ma samples are longer, such as Indus delta Last Glacial Maximum (LGM) sediments that have an AFT central age of 9 ± 1 Ma (Clift *et al.* 2010), is consistent with a dominant Karakoram source.

That the Nd isotope provenance data change at around the same time as the AFT lag times (after 5.7 Ma; Fig. 6) supports the idea that a change in provenance may account for at least part of the changing AFT lag times at that time. The absence of the very short lag time samples does mean that after 5.7 Ma there are no longer any significant fast-eroding ranges in the catchment. As noted above, the Crystalline Inner Lesser Himalaya is known to be experiencing unroofing after ~6 Ma, at least in the vicinity of the Beas River catchment (Najman *et al.* 2009), and the shift in the general character of the AFT age populations after 5.7 Ma may in large part simply reflect more sediment delivery from the Greater and Lesser Himalaya, potentially related to tectonic imbrication and rock uplift (Bollinger *et al.* 2004; Huyghe *et al.* 2001; Webb, 2013). Such a shift is consistent with the evolving provenance data in the Laxmi Basin (Clift *et al.* 2019*b*). The structural reconstructions of Webb (2013) for the western Himalaya propose that both the Greater and Lesser Himalaya remained buried under the Tethyan Himalaya until after 5.4 Ma. This would imply that the source of rapidly cooled grains before that time would be from the Karakoram and Tethyan Himalaya.

The AFT ages can be used to constrain changing rates of exhumation in the bedrock sources. Comparing depositional age against the AFT minimum age populations allows us to assess the lag time between cooling of bedrock sources as they passed through the 60–110 °C PAZ and their final deposition in the deep water of the Indian Ocean (Fig. 6). In our analysis we further compare our results with those similar-aged fluvial sedimentary rocks from the Siwalik Group in western and central Nepal (van der Beek *et al.* 2006), as well as from the Bengal Fan collected by ODP Leg 116 (Corrigan & Crowley, 1990). It is clear that many of these minimum age groups have relatively short lag times, which indicates fast cooling and exhumation of bedrock sources. We note that both the oldest (15.5 Ma) sample from the Laxmi Basin and a slightly younger sample from the Bengal Fan show lag times close to 4 Myr in Middle Miocene time. This would imply exhumation rates of 1.1–1.4 km Myr^{-1} assuming 25–35 °C km^{-1} geothermal gradients.

Unfortunately, we have little information between that time and ~8.5 Ma when the next youngest dateable sandy sediment was deposited and preserved at the drilling sites. Although one of the minimum age groups still lags by ~4.2 Myr, we note that there is some scatter to longer lag times of up to 8.8 Myr between 8.5 and 7.0 Ma and with large uncertainties. Combined zircon U–Pb (40–70 and 70–120 Ma grains) and bulk sediment Nd isotope (ϵ_{Nd} values > −10) provenance data indicate that much of the sediment at that time was derived from the Karakoram (Clift *et al.* 2019*b*). The zircon U–Pb budget over-represents the net flux from the Himalaya because these bedrocks are >2.2 times more fertile with regard to zircon than the Karakoram and Transhimalaya.

After 7.0 Ma, lag times shortened significantly. Three samples from the Laxmi Basin drilling sites are within error of the depositional age between 7.0 and 5.7 Ma, requiring exhumation rates that were so rapid that we are unable to constrain the duration between cooling through the PAZ (60–110 °C) and sedimentation, i.e. lag times close to zero. This implies a maximum rate of cooling in the sources at that time. All three of the fast-cooling samples have

https://doi.org/10.1017/S001675681900092X Published online by Cambridge University Press

accompanying zircon U–Pb ages that show that they continue a trend towards more Himalayan erosion but that there is not a sharp contrast with the sediment deposited before 7.0 Ma. After 5.7 Ma, the change in Nd isotopes is especially marked and implies that a change in provenance may be responsible for the slowing of exhumation rates. Nonetheless, one sample, U1457C-43R-1 55–63 cm, deposited at 5.87 Ma, has a minimum age lag time of 3.13 Myr, longer than the others. This implies that not all sources were supplying large volumes of sediment at all times and that not all bedrock sources were exhuming so quickly.

Although provenance data indicate mostly Karakoram sources, these rapidly cooled grains could also be derived from the Himalayan tectonic units. Zircon U–Pb ages allow us to discriminate between erosion of Karakoram (40–120 Ma) and Himalayan (>300 Ma) sources, the largest sources at that time. However, the zircon ages only apply to these minerals and the provenance cannot be transferred to the apatites. Therefore, we only know that there were rapidly cooling areas between 7.0 and 5.7 Ma, but not which range they are located in. However, because there are large numbers of grains in the minimum age group, it might reasonably be expected that these are derived from bedrock sources that also supply large volumes of other mineral types. Between 7.0 and 5.7 Ma the longest lag time was 3.13 Myr in the sediment deposited at 5.87 Ma. This indicates an average cooling rate of at least 35.1 ± 9.7 °C Myr^{-1}, faster than the cooling rates of 12.5 to 26.1 °C Myr^{-1} between 8.2 and 7.0 Ma. These are faster rates than those recorded in the Siwalik Group from Nepal (van der Beek *et al.* 2006), as well as sparse data from the Bengal Fan (Corrigan & Crowley, 1990), although they are within the uncertainties of the peak rates in Nepal at that time. However, in Nepal the sources must have been Himalayan, not Karakoram. In the youngest part of the section (<4 Ma), which is more dominated by Himalaya erosion (Clift *et al.* 2019*b*), these very short lag times are not visible and are always more than 1.93 Myr, equivalent to approximate exhumation rates of ~2.3–1.6 km Myr^{-1}. The moderate exhumation rates after 4 Ma compare with data from both the Bengal Fan and from the Nepalese part of the Himalayan foreland. Both these sediment sequences are dominated by Himalayan erosion (Bouquillon *et al.* 1990). Slowing of exhumation in the Indus Basin after 5.7 Ma is consistent with data from western Nepal (Karnali), but the slowing from peak rates at 7.0 to 5.7 Ma is in contrast to conclusions of work from central Nepal (Surai and Tinau Khola) that argued for relatively steady-state cooling in that part of the mountain range (van der Beek *et al.* 2006). The very youngest sample deposited at 930 ka stands out as having by far the largest lag time and is inferred to have a unique source, likely a mixture of sediment from the Indus River and Peninsular India.

We can compare this pattern of accelerating exhumation before 7.0 Ma and then slowing after 5.7 Ma with the climatic history (Fig. 6), while recognizing the shift in provenance that is occurring at the same time. One of the most popular long-term proxies for monsoon intensity in the Arabian Sea is the relative abundance of *Globigerina bulloides* offshore the margin of Arabia. The abundance of *G. bulloides* is largely a function of the availability of nutrients derived from upwelling caused by the summer monsoon rains (Curry *et al.* 1992). There is little evidence for such strong upwelling prior to *c.* 13 Ma (Betzler *et al.* 2016). A general intensification of upwelling is noted after 5.3 and 3.0 Ma (Gupta *et al.* 2015; Huang *et al.* 2007) (Fig. 6). However, upwelling is not a direct proxy of rainfall, and this apparent intensification does not reflect the delivery of summer rains to the mountain front, because this proxy does not correlate with other climatically sensitive indicators (Clift, 2017).

Stable oxygen isotope data from the foreland basin instead agree with chemical weathering data from the South China and Arabian Seas in arguing for relatively wet conditions in Middle Miocene time between 10 and 12 Ma (Dettman *et al.* 2001) followed by a decrease in humidity, particularly after *c.* 6–8 Ma (Clift, 2017; Singh *et al.* 2011). Moisture delivery to this area from the winter Westerlies is also reconstructed to reduce *c.* 7 Ma (Vögeli *et al.* 2017). The increasing lag time seen in the minimum age populations after 5.7 Ma would be consistent with slower erosion and could be linked to weaker monsoon rainfall. Weaker monsoon and Westerly rains would also reduce discharge and potentially slow the transport of sediment across the flood plains. Increased aridity is consistent with decreasing strength of chemical weathering seen in Indus Marine A-1 located on the Indus shelf (Clift *et al.* 2008), as well as Site U1456 (Clift *et al.* 2019*a*), but largely postdates the carbon isotope transition from 8 to 6 Ma in the foreland basin (Quade *et al.* 1989).

The acceleration in exhumation rates from 7.8 to 7.0 Ma generally coincides with the climatic drying, which may seem counterintuitive. However, this also assumes that stronger rains, sometimes modulated through glaciation, always increase erosion. There is evidence that drier conditions, especially when this involves heightened seasonality, can increase erosion provided the drying is not too extreme but sufficient to reduce vegetation cover that reduces soil erosion (Giosan *et al.* 2017). There is no evidence that the period of fast erosion at 5.7–7.0 Ma was caused by faster India and Asia convergence. Indeed, convergence rates appear to have slowed gradually during the Cenozoic period (Clark, 2012).

6. Conclusions

Apatite fission track ages derived from turbidite sediments from IODP sites U1456 and U1457 in the Laxmi Basin, eastern Arabian Sea, provide an opportunity to reconstruct changing exhumation rates in the western Himalaya and Karakoram since 15.5 Ma, and especially since 9 Ma. AFT ages are mostly <50 Ma and demonstrate that the sediment is derived from the Indus River, not Peninsular India, except in the case of the youngest sample, deposited at 0.93 Ma. Moreover, most samples show minimum age populations that are only slightly older than the depositional age, implying fast rates of exhumation in the sources and rapid transport through this time. Lag times of ~4 Myr in Middle Miocene time imply exhumation rates of 1.1–1.4 km Myr^{-1}. After a period of longer lag times (~6 Myr) between 8.5 and 7.8 Ma, these reach a minimum from 7.0 to 5.7 Ma, when lag times were within error of zero. Provenance U–Pb zircon and Nd isotope data indicate erosion dominantly in the Karakoram, but the AFT ages could have also come from Himalayan sources, which were also important contributors at this time. The AFT data alone do not allow us to discriminate which of the two ranges contained the fast-exhuming sources. After 5.7 Ma, lag times lengthened to ~4.5 Ma, and exhumation rates slowed to 2.3–1.6 km Myr^{-1} at the same time that sediment supply came progressively more from the Himalaya and relatively less from the Karakoram.

The time of peak exhumation correlates with the transition to a drier climate in the foreland basin and of a weakening Westerly Jet. Erosion rates since 5.7 Ma are comparable or slightly faster than those seen in the Nepalese parts of the Himalaya and the Bengal Fan. Slowing exhumation rates after 5.7 Ma correlate with

https://doi.org/10.1017/S001675681900092X Published online by Cambridge University Press

a drying climate and weaker summer monsoon rains in Late Miocene time. There is a general shift in the AFT age populations from longer lag times, more similar to the glacial era Indus River and associated with dominant erosion in the Karakoram prior to 7 Ma, to shorter lag times and more erosion of the Himalaya, similar to the Holocene Indus River after 5.7 Ma. The acceleration of exhumation as the climate dried between 7.8 and 7.0 Ma seems to imply a dominant tectonic control of erosion. The AFT data support models that imply a non-linear relationship between summer monsoon rain strength and the erosion of the western Himalaya.

Supplementary material. To view supplementary material for this article, please visit https://doi.org/10.1017/S001675681900092X

Acknowledgements. This research used samples and/or data provided by the International Ocean Discovery Program (IODP). Funding for this research was provided by USSSP and the Charles T. McCord Jr Chair in Petroleum Geology at LSU. We thank GeoSep Services and especially Paul O'Sullivan for separation of our apatite grains. The paper was improved by reviews from Peter van der Beek and an anonymous reviewer.

References

Alizai A, Carter A, Clift PD, VanLaningham S, Williams JC and Kumar R (2011) Sediment provenance, reworking and transport processes in the Indus River by U–Pb dating of detrital zircon grains. *Global and Planetary Change* **76**, 33–55. doi: 10.1016/j.gloplacha.2010.11.008.

Baral U, Lin D and Chamlagain D (2016) Detrital zircon U–Pb geochronology of the Siwalik Group of the Nepal Himalaya: implications for provenance analysis. *International Journal of Earth Sciences* **105**, 921–39, doi: 10.1007/s00531-015-1198-7.

Behrensmeyer AK, Quade J, Cerling TE, Kappelman J, Khan IA, Copeland P, Roe L, Hicks J, Stubblefield P, Willis BJ and Latorre C (2007) The structure and rate of late Miocene expansion of C4 plants: Evidence from lateral variation in stable isotopes in paleosols of the Siwalik Group, northern Pakistan. *Geological Society of America Bulletin* **119**, 1486–505. doi: 10.1130/B26064.1.

Bernet M, van der Beek P, Pik R, Huyghe P, Mugnier J-L, Labrin E and Szulc AG (2006) Miocene to Recent exhumation of the central Himalaya determined from combined detrital zircon fission-track and U/Pb analysis of Siwalik sediments, western Nepal. *Basin Research* **18**, 393–412. doi: 10.1111/j.1365-2117.2006.00303.

Betzler C, Eberli GP, Kroon D, Wright JD, Swart PK, Nath BN, Alvarez-Zarikian CA, Alonso-García M, Bialik OM, Blättler CL, Guo JA, Haffen S, Horozai S, Inoue M, Jovane L, Lanci L, Laya JC, Mee ALH, Lüdmann T, Nakakuni M, Niino K, Petruny LM, Pratiwi SD, Reijmer JJG, Reolid J, Slagle AL, Sloss CR, Su X, Yao Z and Young JR (2016) The abrupt onset of the modern South Asian monsoon winds. *Scientific Reports* **6**, 29838. doi: 10.1038/srep29838.

Bhattacharya GCB, Chaubey AK, Murty GPS, Srinivas S, Sarma KV, Subrahmanyam V and Krishna KS (1994) Evidence for seafloor spreading in the Laxmi Basin, northeastern Indian Ocean. *Earth and Planetary Science Letters* **125**, 211–20.

Bollinger L, Avouac JP, Beyssac O, Catlos EJ, Harrison TM, Grove M, Goffe B and Sapkota S (2004) Thermal structure and exhumation history of the Lesser Himalaya in central Nepal. *Tectonics* **23**, 19. doi: 10.1029/2003TC001564.

Bookhagen B and Burbank DW (2006) Topography, relief, and TRMM-derived rainfall variations along the Himalaya. *Geophysical Research Letters* **33** L08405. doi: 10.1029/2006GL026037.

Bouquillon A, France-Lanord C, Michard A and Tiercelin J (1990) Sedimentology and isotopic chemistry of the Bengal Fan sediments: the denudation of the Himalaya. In *Proceedings of the Ocean Drilling Program, Scientific Results, vol. 116* (eds JR Cochran, DAV Stow and C Auroux), pp. 43–58. College Station, Texas.

Calvès G, Huuse M, Clift PD and Brusset S (2015) Giant fossil mass wasting off the coast of West India: the Nataraja submarine slide. *Earth and Planetary Science Letters* **432**, 265–72. doi: 10.1016/j.epsl.2015.10.022.

Carter A (1999) Present status and future avenues of source region discrimination and characterization using fission track analysis. *Sedimentary Geology* **124**, 31–45. doi: 10.1016/S0037-0738(98)00119-5.

Carter A (2007) Heavy minerals and detrital fission-track thermochronology. *Developments in Sedimentology* **58**, 851–68. doi: 10.1016/S0070-4571(07)58033-7.

Cerveny PF, Johnson NM, Tahirkheli RAK and Bonis NR (1989) Tectonic and geomorphic implications of Siwalik Group heavy minerals, Potwar Plateau, Pakistan. In *Tectonics of the Western Himalayas* (eds LL Malinconico and RJ Lillie), pp. 129–36. Boulder, Colorado: Geological Society of America Special Paper no. 232.

Chirouze F, Huyghe P, Chauvel C, van der Beek P, Bernet M and Mugnier J-L (2015) Stable drainage pattern and variable exhumation in the Western Himalaya since the Middle Miocene. *Journal of Geology* **123**, 1–20. doi: 10.1086/679305.

Chirouze F, Huyghe P, van der Beek P, Chauvel C, Chakraborty T, Dupont-Nivet G and Bernet M (2013) Tectonics, exhumation, and drainage evolution of the eastern Himalaya since 13 Ma from detrital geochemistry and thermochronology, Kameng River Section, Arunachal Pradesh. *Geological Society of America Bulletin* **125**, 523–38.

Clark MK (2012) Continental collision slowing due to viscous mantle lithosphere rather than topography. *Nature* **483**, 74–7. doi: 10.1038/nature10848.

Clift PD (2006) Controls on the erosion of Cenozoic Asia and the flux of clastic sediment to the ocean. *Earth and Planetary Science Letters* **241**, 571–80.

Clift PD (2017) Cenozoic sedimentary records of climate-tectonic coupling in the Western Himalaya. *Progress in Earth and Planetary Science* **4**, 1–22. doi: 10.1186/s40645-017-0151-8.

Clift PD and Blusztajn JS (2005) Reorganization of the western Himalayan river system after five million years ago. *Nature* **438**, 1001–3.

Clift PD, Campbell IH, Pringle MS, Carter A, Zhang X, Hodges KV, Khan AA and Allen CM (2004) Thermochronology of the modern Indus River bedload; new insight into the control on the marine stratigraphic record. *Tectonics* **23**, 1–17. doi: 10.1029/2003TC001559.

Clift PD, Carter A, Krol M and Kirby E (2002a) Constraints on India; Eurasia collision in the Arabian Sea region taken from the Indus Group, Ladakh Himalaya, India. In *The Tectonic and Climatic Evolution of the Arabian Sea Region* (eds PD Clift, D Kroon, C Gaedicke and J Craig), pp. 97–116. Geological Society of London, Special Publication no. 195.

Clift PD and Giosan L (2014) Sediment fluxes and buffering in the post-glacial Indus Basin. *Basin Research* **26**, 369–86. doi: 10.1111/bre.12038.

Clift PD, Giosan L, Carter A, Garzanti E, Galy V, Tabrez AR, Pringle M, Campbell IH, France-Lanord C, Blusztajn J, Allen C, Alizai A, Lückge A, Danish M and Rabbani MM (2010) Monsoon control over erosion patterns in the Western Himalaya: possible feed-backs into the tectonic evolution. In *Monsoon Evolution and Tectonic-Climate Linkage in Asia* (eds PD Clift, R Tada and H Zheng), pp. 181–213. Geological Society of London, Special Publication no. 342.

Clift PD, Hodges K, Heslop D, Hannigan R, Hoang LV and Calves G (2008) Greater Himalayan exhumation triggered by Early Miocene monsoon intensification. *Nature Geoscience* **1**, 875–80. doi: 10.1038/ngeo351.

Clift PD, Kulhanek DK, Zhou P, Bowen MG, Vincent SM, Lyle M and Hahn A (2019a) Chemical weathering and erosion responses to changing monsoon climate in the late Miocene of Southwest Asia. *Geological Magazine*, published online 13 June 2019. doi: 10.1017/S0016756819000608.

Clift PD, Lee JI, Hildebrand P, Shimizu N, Layne GD, Blusztajn J, Blum JD, Garzanti E and Khan AA (2002b) Nd and Pb isotope variability in the Indus River system; implications for sediment provenance and crustal heterogeneity in the western Himalaya. *Earth and Planetary Science Letters* **200**, 91–106. doi: 10.1016/S0012-821X(02)00620-9.

Clift PD, Shimizu N, Layne G, Gaedicke C, Schlüter HU, Clark MK and Amjad S (2001) Development of the Indus Fan and its significance for the erosional history of the western Himalaya and Karakoram. *Geological Society of America Bulletin* **113**, 1039–51.

Clift PD, Zhou P, Stockli DF and Blusztajn J (2019b) Regional Pliocene exhumation of the Lesser Himalaya in the Indus drainage. *Solid Earth* **10**, 647–61. doi: 10.5194/se-10-647-2019.

Corrigan JD and Crowley JL (1990) Fission track analysis of detrital apatites from Sites 717 and 718, leg 116, central Indian Ocean. In *Proceedings of the Ocean Drilling Program, Scientific Results, vol. 116* (eds JR Cochran and DAV Stow), pp. 75–92. College Station, Texas.

Curry WB, Ostermann DR, Guptha MVS and Itekkot V (1992) Foraminiferal production and monsoonal upwelling in the Arabian Sea; evidence from sediment traps. In *Upwelling Systems; Evolution Since the Early Miocene* (eds CP Summerhayes, WL Prell and KC Emeis), pp. 93–106. Geological Society of London, Special Publication no. 64.

Dailey SK, Clift PD, Kulhanek DK, Blusztajn J, Routledge CM, Calvès G, O'Sullivan, P, Jonell TN, Pandey DK, Andò S, Coletti G, Zhou P, Li Y, Neubeck NE, Bendle JAP, Bratenkov S, Griffith EM, Gurumurthy GP, Hahn A, Iwai M, Khim B-K, Kumar A, Kumar AG, Liddy HM, Lu H, Lyle MW, Mishra R, Radhakrishna T, Saraswat R, Saxena R, Scardia G, Sharma GK, Singh AD, Steinke S, Suzuki K, Tauxe L, Tiwari M, Xu Z and Yu Z (2019) Large-scale mass wasting on the Miocene continental margin of Western India. *Geological Society of America Bulletin*, published online 9 May 2019. doi: 10.1130/B35158.1.

DeCelles PG, Kapp P, Gehrels GE and Ding L (2014) Paleocene-Eocene foreland basin evolution in the Himalaya of southern Tibet and Nepal: implications for the age of initial India-Asia collision. *Tectonics* **33**, 824–49. doi: 10.1002/ 2014TC003522.

Dettman DL, Kohn MJ, Quade J, Ryerson FJ, Ojha TP and Hamidullah S (2001) Seasonal stable isotope evidence for a strong Asian monsoon throughout the past 10.7 m.y. *Geology* **29**, 31–4.

Dietze M, Kreutzer S, Burow C, Fuchs MC, Fischer M and Schmidt C (2016) The abanico plot: visualising chronometric data with individual standard errors. *Quaternary Geochronology* **31**, 12–18. doi: 10.1016/j.quageo.2015.09.003.

Foster DA, Gleadow AJW and Mortimer G (1994) Rapid Pliocene exhumation in the Karakoram (Pakistan), revealed by fission-track thermochronology of the K2 gneiss. *Geology* **22**, 19–22.

Galbraith RF (1990) The radial plot: graphical assessment of spread in ages. *Nuclear Tracks and Radiation Measurement* **17**, 207–14.

Galbraith RF (2005) *Statistics for Fission Track Analysis*. Boca Raton, FL: CRC Press.

Galbraith RF and Green PF (1990) Estimating the component ages in a finite mixture. *Nuclear Tracks and Radiation Measurement* **17**, 197–206.

Gallagher K, Hawkesworth CJ and Mantovani MSM (1995) Denudation, fission track analysis and the long-term evolution of passive margin topography: application to the S.E. Brazilian margin. *Journal of South American Earth Sciences* **8**, 65–77.

Garzanti E, Vezzoli G, Ando S, France-Lanord C, Singh SK and Foster G (2004) Sand petrology and focused erosion in collision orogens: the Brahmaputra case. *Earth and Planetary Science Letters* **220**, 157–74.

Garzanti E, Vezzoli G, Ando S, Paparella P and Clift PD (2005) Petrology of Indus River sands; a key to interpret erosion history of the western Himalayan syntaxis. *Earth and Planetary Science Letters* **229**, 287–302. doi: 10.1016/j.epsl.2004.11.008.

Ghosh SK and Kumar R (2000) Petrography of Neogene Siwalik sandstone of the Himalayan foreland basin, Garhwal Himalaya: Implications for source area tectonics and climate. *Journal of the Geological Society of India* **55**, 1–15.

Giosan L, Ponton C, Usman M, Blusztajn J, Fuller DQ, Galy V, Haghipour N, Johnson JE, McIntyre C, Wacker L and Eglinton TI (2017) Short communication: massive erosion in monsoonal central India linked to late Holocene land cover degradation. *Earth Surface Dynamics* **5**, 781–9. doi:10.5194/esurf-5-781-2017.

Green PF (1989) Thermal and tectonic history of the East Midlands shelf (onshore UK) and surrounding regions assessed by apatite fission track analysis. *Journal of the Geological Society, London* **146**, 755–73.

Green PF, Duddy IR, Laslett GM, Hegarty KA, Gleadow AJW and Lovering JF (1989) Thermal annealing of fission tracks in apatite; 4, Quantitative modelling techniques and extension to geological timescales. *Chemical Geology: Isotope Geoscience section* **79**, 155–82.

Gunnell Y, Gallagher K, Carter A, Widdowson M and Hurford AJ (2003) Denudation history of the continental margin of western peninsular India since early Mesozoic—reconciling apatite fission track data with geomorphology. *Earth and Planetary Science Letters* **215**, 187–201.

Gupta AK, Yuvaraja A, Prakasam M, Clemens SC and Velu A (2015) Evolution of the South Asian monsoon wind system since the late Middle Miocene. *Palaeogeography, Palaeoclimatology, Palaeoecology* **438**, 160–7. doi:10.1016/j.palaeo.2015.08.006.

Haack U (1977) The closing temperature for fission track retention in minerals. *American Journal of Science* **277**, 459–64.

Huang Y, Clemens SC, Liu W, Wang Y and Prell WL (2007) Large-scale hydrological change drove the late Miocene C4 plant expansion in the Himalayan foreland and Arabian Peninsula. *Geology* **35**, 531–4.

Hurford A (1990) Standardization of fission track dating calibration: recommendation by the Fission Track Working Group of the IUGS Subcommission on Geochronology. *Chemical Geology* **80**, 177–8.

Huyghe P, Galy A, Mugnier J-L and France-Lanord C (2001) Propagation of the thrust system and erosion in the Lesser Himalaya: geochemical and sedimentological evidence. *Geology* **29**, 1007–10.

Jain AK, Kumar D, Singh S, Kumar A and Lal N (2000) Timing, quantification and tectonic modelling of Pliocene–Quaternary movements in the NW Himalaya; evidence from fission track dating. *Earth and Planetary Science Letters* **179**, 437–51.

Kalaswad S, Roden MK, Miller DS and Morisawa M (1993) Evolution of the continental margin of western India: new evidence from apatite fission-track dating. *Journal of Geology* **101**, 667–73.

Kirstein LA, Foeken JPT, van der Beek P, Stuart FM and Phillips RJ (2009) Cenozoic unroofing history of the Ladakh Batholith, western Himalaya constrained by thermochronology and numerical modeling. *Journal of the Geological Society, London* **166**, 667–78. doi: 10.1144/0016-7649.2008-107.

Kirstein LA, Sinclair HD, Stuart FM and Dobson K (2006) Rapid early Miocene exhumation of the Ladakh batholith, western Himalaya. *Geology* **34**, 1049–52. doi: 10.1130/G22857A

Krol MA, Zeitler PK and Copeland P (1996) Episodic unroofing of the Kohistan Batholith, Pakistan: implications from K-feldspar thermochronology. *Journal of Geophysical Research–Solid Earth* **101**, 28149–64.

Kroon D, Steens T and Troelstra SR (1991) Onset of monsoonal related upwelling in the western Arabian Sea as revealed by planktonic foraminifers. In *Proceedings of the Ocean Drilling Program, Scientific Results, vol. 117* (eds W Prell and N Niitsuma), pp. 257–63. College Station, Texas.

Kumar A, Lal N, Jain AK and Sorkhabi RB (1995) Late Cenozoic–Quaternary thermo-tectonic history of Higher Himalayan Crystalline (HHC) in Kishtwar-Padar-Zanskar region, NW Himalaya; evidence from fission track ages. *Journal of the Geological Society of India* **45**, 375–91.

Laslett GM, Green PF, Duddy IR and Gleadow AJW (1987) Thermal annealing of fission track grains in apatite. *Chemical Geology* **65**, 1–13.

Lavé J and Avouac JP (2001) Fluvial incision and tectonic uplift across the Himalaya of central Nepal. *Journal of Geophysical Research* **106**, 26561–91. doi: 10.1029/2001JB000359.

Lee JI, Clift PD, Layne G, Blum J and Khan AA (2003) Sediment flux in the modern Indus River traced by the trace element composition of detrital amphibole grains. *Sedimentary Geology* **160**, 243–57. doi: 10.1016/S0037-0738(02)00378-0.

Li Y, Clift PD and O'Sullivan P (2019) Millennial and centennial variations in zircon U–Pb and apatite fission track ages in the Quaternary Indus submarine canyon. *Basin Research* **31**, 155–70. doi: 10.1111/bre.12313.

Li G, Tian Y, Kohn BP, Sandiford M, Xu Z and Cai Z (2015) Cenozoic low temperature cooling history of the Northern Tethyan Himalaya in Zedang, SE Tibet and its implications. *Tectonophysics* **643**, 80–93. doi: 10.1016/j.tecto.2014.12.014.

Meigs AJ, Burbank DW and Beck RA (1995) Middle-late Miocene (>10 Ma) formation of the Main Boundary thrust in the western Himalaya. *Geology* **23**, 423–6.

Métivier F, Gaudemer Y, Tapponnier P and Klein M (1999) Mass accumulation rates in Asia during the Cenozoic. *Geophysical Journal International* **137**, 280–318.

Miles PR and Roest WR (1993) Earliest seafloor spreading magnetic anomalies in the north Arabian Sea and the ocean-continent transition. *Geophysical Journal International* **115**, 1025–31.

Mishra R, Pandey DK, Ramesh P and Clift PD (2016) Identification of new deep sea sinuous channels in the eastern Arabian Sea. *SpringerPlus* **5**, 844. doi: 10.1186/s40064-016-2497-6.

Mugnier J-L, Huyghe P, Chalaron E and Mascle G (1994) Recent movements along the Main Boundary Thrust of the Himalayas: normal faulting in an over-critical thrust wedge? *Tectonophysics* **238**, 199–215.

Najman Y (2006) The detrital record of orogenesis: a review of approaches and techniques used in the Himalayan sedimentary basins. *Earth-Science Reviews* **74**, 1–72.

Najman Y, Appel E, Boudagher-Fadel M, Bown P, Carter A, Garzanti E, Godin L, Han J, Liebke U, Oliver G, Parrish R and Vezzoli G (2010) Timing of India-Asia collision: Geological, biostratigraphic, and palaeomagnetic constraints. *Journal of Geophysical Research* **115**, 1–18. doi: 10.1029/2010JB007673.

Najman Y, Bickle M, Garzanti E, Pringle M, Barfod D, Brozovic N, Burbank D and Ando S (2009) Reconstructing the exhumation history of the Lesser Himalaya, NW India, from a multitechnique provenance study of the foreland basin Siwalik Group. *Tectonics* **28**, 1–15. doi: 10.1029/2009TC002506.

Pandey DK, Clift PD, Kulhanek DK, Andò S, Bendle JAP, Bratenkov S, Griffith EM, Gurumurthy GP, Hahn A, Iwai M, Khim B-K, Kumar A, Kumar AG, Liddy HM, Lu H, Lyle MW, Mishra R, Radhakrishna T, Routledge CM, Saraswat R, Saxena R, Scardia G, Sharma GK, Singh AD, Steinke S, Suzuki K, Tauxe L, Tiwari M, Xu Z and Yu Z (2016a) Site U1456. In *Arabian Sea Monsoon. Proceedings of the International Ocean Discovery Program, vol. 355* (eds DK Pandey, PD Clift and DK Kulhanek), pp. 1–61. College Station, Texas. doi: 10.14379/iodp.proc.355.103.2016.

Pandey DK, Clift PD, Kulhanek DK, Andò S, Bendle JAP, Bratenkov S, Griffith EM, Gurumurthy GP, Hahn A, Iwai M, Khim B-K, Kumar A, Kumar AG, Liddy HM, Lu H, Lyle MW, Mishra R, Radhakrishna T, Routledge CM, Saraswat R, Saxena R, Scardia G, Sharma GK, Singh AD, Steinke S, Suzuki K, Tauxe L, Tiwari M, Xu Z and Yu Z (2016b) Expedition 355 summary. In *Arabian Sea Monsoon. Proceedings of the International Ocean Discovery Program, vol. 355* (eds DK Pandey, PD Clift and DK Kulhanek), pp. 1–32. College Station, Texas. doi: 10.14379/iodp.proc.355.101.2016.

Pandey OP, Agrawal PK and Negi JG (1995) Lithospheric structure beneath Laxmi Ridge and late Cretaceous geodynamic events. *Geo-Marine Letters* **15**, 85–91.

Poupeau G, Pecher A, Benharbit M and Noyan OF (1991) Ages traces de fission sur apatites et taux de denudation plio-quaternaires au Karakorum central. *Comptes Rendus de l'Academie des Sciences, Serie II Sciences de la Terre et des Planetes* **313**, 917–22.

Prell WL, Murray DW, Clemens SC and Anderson DM (1992) Evolution and variability of the Indian Ocean Summer Monsoon: evidence from the western Arabian Sea drilling program. In *Synthesis of Results from Scientific Drilling in the Indian Ocean* (eds RA Duncan, DK Rea, RB Kidd, U von Rad and JK Weissel), pp. 447–69. American Geophysical Union, Geophysical Monograph vol. 70. Washington, DC, USA.

Quade J, Cerling TE and Bowman JR (1989) Development of Asian monsoon revealed by marked ecological shift during the latest Miocene in northern Pakistan. *Nature* **342**, 163–6.

Sadler PM and Jerolmack DJ (2014) Scaling laws for aggradation, denudation and progradation rates: the case for time-scale invariance at sediment sources and sinks. In *Strata and Time: Probing the Gaps in Our Understanding* (eds DG Smith, RJ Bailey, PM Burgess and AJ Fraser). Geological Society of London, Special Publication no. 404.

Searle MP (1996) Cooling history, erosion, exhumation and kinematics of the Himalaya-Karakoram-Tibet orogenic belt. In *The Tectonic Evolution of Asia* (eds A Yin and TM Harrison), pp. 110–37. Cambridge: Cambridge University Press.

Singh S, Parkash B, Awasthi AK and Kumar S (2011) Late Miocene record of palaeovegetation from Siwalik palaeosols of the Ramnagar sub-basin, India. *Current Science* **100**, 213–22.

Stewart RJ, Hallet B, Zeitler PK, Malloy MA, Allen CM and Trippett D (2008) Brahmaputra sediment flux dominated by highly localized rapid erosion from the easternmost Himalaya. *Geology* **36**, 711–14. doi: 10.1130/G24890A1.

Szulc AG, Najman Y, Sinclair HD, Pringle M, Bickle M, Chapman H, Garzanti E, Ando S, Huyghe P, Mugnier J-L, Ojha T and DeCelles PG (2006) Tectonic evolution of the Himalaya constrained by detrital $^{40}Ar/^{39}Ar$, Sm/Nd and petrographic data from the Siwalik foreland basin succession, SW Nepal. *Basin Research* **18**, 375–91.

Thiede RC, Bookhagen B, Arrowsmith JR, Sobel ER and Strecker MR (2004) Climatic control on rapid exhumation along the Southern Himalayan Front. *Earth and Planetary Science Letters* **222**, 791–806.

van der Beek P, Robert X, Mugnier J-L, Bernet M, Huyghe P and Labrin E (2006) Late Miocene–Recent exhumation of the central Himalaya and recycling in the foreland basin assessed by apatite fission-track thermochronology of Siwalik sediments, Nepal. *Basin Research* **18**, 413–34. doi:10.1111/j.1365-2117.2006.00305.x.

van der Beek P, Van Melle J, Guillot S, Pêcher A, Reiners PW, Nicolescu S and Latif M (2009) Eocene Tibetan plateau remnants preserved in the northwest Himalaya. *Nature Geoscience* **2**, 364–8. doi: 10.1038/NGEO503.

Vannay J-C, Grasemann B, Rahn M, Frank W, Carter A, Baudraz V and Cosca M (2004) Miocene to Holocene exhumation of metamorphic crustal wedges in the NW Himalaya; evidence for tectonic extrusion coupled to fluvial erosion. *Tectonics* **23**. doi: 10.1029/2002TC001429.

Vermeesch P (2012) On the visualisation of detrital age distributions. *Chemical Geology* **312–313**, 190–4. doi: 10.1016/j.chemgeo.2012.04.021.

Vögeli N, Najman Y, Beek PVD, Huyghe P, Wynn PM, Govin G, Veen IVD and Sachse D (2017) Lateral variations in vegetation in the Himalaya since the Miocene and implications for climate evolution. *Earth and Planetary Science Letters* **471**, 1–9. doi: 10.1016/j.epsl.2017.04.037.

Wallis D, Carter A, Phillips RJ, Parsons AJ and Searle MP (2016) Spatial variation in exhumation rates across Ladakh and the Karakoram: new apatite fission track data from the Eastern Karakoram, NW India. *Tectonics* **35**, 704–21. doi: 10.1002/2015TC003943.

Warner LF (1993) *Variable Denudation of the Nanga Parbat-Haramosh Massif: A Fission Track Study of the Tato Valley, Pakistan*. Bethlehem, PA: Lehigh University. 34 pp.

Wasson RJ (2003) A sediment budget for the Ganga–Brahmaputra catchment. *Current Science* **84**, 1041–7.

Webb AAG (2013) Preliminary palinspastic reconstruction of Cenozoic deformation across the Himachal Himalaya (northwestern India). *Geosphere* **9**, 572–87.

White NM, Pringle M, Garzanti E, Bickle M, Najman Y, Chapman H and Friend P (2002) Constraints on the exhumation and erosion of the High Himalayan Slab, NW India, from foreland basin deposits. *Earth and Planetary Science Letters* **195**, 29–44.

Willenbring JK and von Blanckenburg F (2010) Long-term stability of global erosion rates and weathering during late-Cenozoic cooling. *Nature* **465**, 211–14. doi: 10.1038/nature09044.

Zeilinger G, Burg JP, Schaltegger U and Seward D (2001) New U/Pb and fission track ages and their implication for the tectonic history of the lower Kohistan Arc Complex, northern Pakistan. *Journal of Asian Earth Sciences* **19**, 79–81.

Zeitler PK (1985) Cooling history of the NW Himalaya, Pakistan. *Tectonics* **4**, 127–51.

Zeitler PK, Chamberlain CP and Smith HA (1993) Synchronous anatexis, metamorphism, and rapid denudation at Nanga-Parbat (Pakistan Himalaya). *Geology* **21**, 347–50.

Zeitler PK, Sutter JF, Williams IS, Zartman RE and Tahirkheli RAK (1989) Geochronology and temperature history of the Nanga Parbat-Haramosh Massif, Pakistan. In *Tectonics of the Western Himalayas* (eds LL Malinconico and RJ Lillie), pp. 1–22. Boulder, CO: Geological Society of America, Special Paper vol. 232.

Zhang P, Molnar P and Downs WR (2001) Increased sedimentation rates and grain sizes 2–4 Myr ago due to the influence of climate change on erosion rates. *Nature* **410**, 891–7.

Zhuang G, Najman Y, Tian Y, Carter A, Gemignani L, Wijbrans J, Jan MQ and Khan MA (2018) Insights into the evolution of the Hindu Kush-Kohistan-Karakoram from modern river sand detrital geo- and thermochronological studies, London. *Journal of the Geological Society* **175**, 934–48. doi: 10.1144/jgs2018-007.